NASA TECHNICAL MEMORANDUM

NASA TM X-3044

NASA TM X-3044

ELECTRIC ARC DISCHARGE DAMAGE TO ION THRUSTER GRIDS

by Dale D. Beebe, Shigeo Nakanishi, and Robert C. Finke

Lewis Research Center
Cleveland, Ohio 44135

NATIONAL AERONAUTICS AND SPACE ADMINISTRATION • WASHINGTON, D. C. • MAY 1974

1. Report No. NASA TM X-3044	2. Government Accession No.	3. Recipient's Catalog No.
4. Title and Subtitle ELECTRIC ARC DISCHARGE DAMAGE TO ION THRUSTER GRIDS		5. Report Date May 1974 6. Performing Organization Code
7. Author(s) Dale D. Beebe, Shigeo Nakanishi, and Robert C. Finke		8. Performing Organization Report No. E-7767
9. Performing Organization Name and Address Lewis Research Center National Aeronautics and Space Administration Cleveland, Ohio 44135		10. Work Unit No. 502-04 11. Contract or Grant No.
12. Sponsoring Agency Name and Address National Aeronautics and Space Administration Washington, D.C. 20546		13. Type of Report and Period Covered Technical Memorandum 14. Sponsoring Agency Code

15. Supplementary Notes

16. Abstract

Arcs representative of those occurring between the grids of a mercury ion thruster were simulated. Parameters affecting an arc and the resulting damage were studied. The parameters investigated were arc energy, arc duration, and grid geometry. Arc attenuation techniques were also investigated. Potentially serious damage occurred at all energy levels representative of actual thruster operating conditions. Of the grids tested, the lowest open-area configuration sustained the least damage for given conditions. At a fixed energy level a long duration discharge caused greater damage than a short discharge. Attenuation of arc current using various impedances proved to be effective in reducing arc damage. Faults were also deliberately caused using chips of sputtered materials formed during the operation of an actual thruster. These faults were cleared with no serious grid damage resulting using the principles and methods developed in this study.

17. Key Words (Suggested by Author(s))	18. Distribution Statement
Accelerator grid; Electric propulsion; Ion; Mercury; Potential; Thruster	Unclassified - unlimited Category 28

19. Security Classif. (of this report)	20. Security Classif. (of this page)	21. No. of Pages	22. Price*
Unclassified	Unclassified	35	$3.25

* For sale by the National Technical Information Service, Springfield, Virginia 22151

ELECTRIC ARC DISCHARGE DAMAGE TO ION THRUSTER GRIDS

by Dale D. Beebe, Shigeo Nakanishi, and Robert C. Finke

Lewis Research Center

SUMMARY

Arcs representative of those occurring between the grids of a mercury ion thruster were simulated. Parameters affecting an arc and the resulting damage were studied. Parameters investigated were arc energy, arc duration, and grid geometry. Arc attenuation techniques were also investigated. Potentially serious damage occurred at all energy levels representative of actual thruster operating conditions. Of the grids tested, the lowest open area configuration sustained the least damage for given conditions. At a fixed energy level, a long duration discharge caused greater damage than a short discharge. Attenuation of arc current using various impedances proved to be effective in reducing arc damage. Faults were also deliberately caused using chips of sputtered materials formed during the operation of an actual thruster. These faults were cleared with no serious grid damage resulting using the principles and methods developed in this study.

INTRODUCTION

A satellite in synchronous orbit requires small thrusters for attitude control and stationkeeping. Electric ion thrusters with millinewton thrust are very attractive for these functions on a satellite with a mission of 5 to 10 years because equivalent gas expulsion systems require propellant masses up to 20 percent of the vehicle mass (ref. 1). The mercury electron bombardment thruster has been developed in an 8-centimeter version for these applications, with design emphasis being placed on reliability and stability (ref. 2).

An accelerating potential of approximately 1200 volts is necessary to obtain the specific impulse required by these mission applications. High-voltage arcs may occur between the accelerating electrodes if they become thermally distorted or are shorted by sputtered metallic flakes. These high-voltage arcs may extinguish the thruster discharge (ref. 3) and may cause damage to thruster components. Such effects must be

minimized in order to retain thruster reliability and lifetime.

The purpose of this investigation was to determine the relation between high-voltage power supply characteristics and their effects on arc transients and the resulting thruster grid surface damage.

Grid arcing was simulated under controlled conditions, and the damage was evaluated. The parameters varied were the amount of energy discharged, the grid geometry, and the duration of the discharge. The damage was thus related to the power supply characteristics and the grid configuration. Finally, methods of attenuating such arcs were investigated.

Preventing or minimizing arc damage to thruster grids is of particular concern because high-performance thrusters require very thin screen grids with narrow webs. The results of these experiments can serve as guidelines in the design of power processors and grid configurations for ion thrusters. These experiments are also pertinent to the problem of clearing grid faults. When a thruster grid system is shorted by a metallic flake of sputtered material, this particle must be vaporized without damaging the grids for recovery of normal thruster operation.

APPARATUS AND PROCEDURE

Standard Test Methods

A typical 8-centimeter mercury electron-bombardment-thruster grid system is shown in figure 1. The closely spaced screen and accelerator grid structure is indicated by the arrow. Figure 2 is a simplified electrical schematic diagram showing the connection points of the high-voltage power supplies. A negative accelerator potential V_A is applied directly to the accelerator grid. The positive net accelerating potential V_I is applied to the anode of the ionization chamber. The screen grid is electrically connected to the thruster body and the cathode is 35 to 45 volts negative with respect to the anode by virtue of the discharge voltage, ΔV_I.

The high-voltage system in this experiment was a capacitor bank charged to thruster potentials through a resistance large enough to provide adequate isolation from the power supply. Samples of dished grid pairs connected to the capacitors were pushed together until an arc occurred. The simulation did not include the ion-chamber discharge plasma and was done in an atmospheric environment.

All grid samples used in the experiment were 1.5-centimeter-diameter molybdenum dished (convex) grids. The holes were etched into the material, 50 percent from each side. Dished grids pairs were used because modern high-performance thrusters used such a configuration. The grids were attached to heavy conductors, 1.90 centimeters

wide and 0.130 centimeter thick, with silver solder to minimize circuit resistance.

Each grid pair was subjected to 20 arcs. This procedure was adopted because it was sometimes difficult to detect the damage due to one arc. The potentials used covered a range from 500 to 3000 volts, which are representative of grid potentials in an operating thruster. The apparatus used in these tests is shown in figure 3. The mechanism used to push the grids together consisted of a screw driven by a slow speed motor. The screw moved an insulated rod at a measured rate of 2.5×10^{-5} meter per second. The drive motor was reversed immediately after each arc. One of the conductors attached to the grids passed through a current transformer connected to an oscilloscope for making an oscillograph of the current waveform. The grids were then examined microscopically and photomicrographs were taken of the most seriously damaged spots using appropriate magnification.

Arc Damage Tests

Energy level. - Using the apparatus of figure 3 and in the preceding section Standard Test Methods, a series of tests were conducted to study grid damage as a function of the energy (initially stored in the capacitor bank) dissipated in the arc discharge. The values of capacitance used ranged from 0.25 to 8 microfarad, which are representative of output circuit capacitors used in high-voltage power supplies for ion thrusters. Two voltages were used in each case, 1500 and 3000 volts.

Grid geometries. - Three types of grid geometries were used in this experiment. They will be referred to as types 1, 2, and 3, described as follows:

Type 1

Grid material	Molybdenum
Grid thickness, cm	0.038
Hole shape	Circle
Hole diameter, cm	0.190
Center-to-center hole spacing, cm	0.254
Open area, percent	51

Type 2

Grid material	Molybdenum
Grid thickness, cm	0.0305
Hole shape	Hexagon
Hole size, (face to face), cm	0.208
Center-to-center hole spacing, cm	0.254
Open area, percent	75

Type 3

Grid material	Molybdenum
Grid thickness, cm	0.038
Hole shape	Hexagon
Hole size (face to face), cm	0.203
Center-to-center hole spacing, cm	0.234
Open area, percent	78

To determine the relative severity of arc damage, all three types of grids were subjected to arcs with fixed initial conditions of voltage and capacitance. The capacitor used was 8 microfarads and was charged to 1500 volts and 2.2 megohms. Oscillographs were taken, and the damage was evaluated as previously described.

Arc duration. - Tests were conducted to determine the dependence of grid damage on the duration of the arc. At a fixed energy level of 1 joule, one set of grids was subjected to a fast arc (lasting about 1 μsec) using a 0.25-microfarad capacitor charged to 2.83 kilovolts. A second set of grids was subjected to a slower arc (lasting about 30 μsec) using an 8-microfarad capacitor charged to 500 volts. Grid material type 2 was used in both tests.

Arc Characteristics Tests

Thruster simulation. - The atmospheric simulation of the thruster grid system did not include the ion chamber plasma discharge operating in vacuum. To establish the validity of the tests performed under atmospheric conditions, an arc having the same initial conditions of voltage and capacitance as in the air test was established between grids in a simulated thruster low-pressure mercury vapor environment. The apparatus used in these thruster arc simulation tests is shown in figure 4. A flask with a pool of mercury in the bottom was kept at 0° C by means of an ice bath. At 0° C the vapor pressure of mercury is 2.5×10^{-4} newton per square meter (1.9×10^{-4} torr), which is near the estimated pressure at the grids of an operating thruster (ref. 3). The flask was sealed with a rubber stopper through which two copper tubes passed to support the grids, the rubber stopper allowed the electrodes enough movement to open and close the grid-to-grid gap. An 8-microfarad capacitor was charged to 1500 volts through a 270 000-ohm resistor. The grids were then slowly brought together until an arc occurred in the gap between them. This test was repeated at atmospheric pressure. In both cases oscillograph traces of the current pulses through the arc were made and compared.

In the second set of thruster arc simulation tests, the grids were examined for damage after being subjected to 20 pulses from a 4-microfarad capacitor charge to 500 volts. This test was repeated at atmospheric pressure. Damage was evaluated and compared

according to the Standard Test Methods section.

Reproducibility. - Another test was performed to check the reproducibility of the experimental methods. Grid erosion could possibly cause individual arcs to have different characteristics invalidating any comparison between arc current waveforms going through the same set of grids. A set of grids was arced 20 times, and an oscillograph was taken of the 1st, 10th, and 20th current waveform during arcing. The waveforms were compared to see if there was any change of arc characteristics.

Attenuation methods. - In an attempt to minimize the damaging effects of arcs, various impedances were placed in series with the grids. An 8-microfarad capacitor was charged to 1000 volts and in separate tests was discharged through the circuits formed by the grids, busbars, and a series impedance.

The impedances used were

(1) A short circuit

(2) A 60-millihenry, 250-ohm choke

(3) A 250-ohm noninductive resistor

(4) A 5-henry, 300-ohm choke

(5) A 300-ohm noninductive resistor.

To cause the discharge in these tests, a pool of mercury was raised beneath a set of contacts until an arc occurred. This apparatus is shown in figure 5. Oscillograph traces were taken of the current pulses and compared in each case.

Chip Clearing Test

Chips of sputtered metal obtained from the discharge chambers of operating thrusters were dropped between a set of grids in air at operating potentials in order to simulate grid faults. The power supply connected to the grid had a 50 milliampere overcurrent trip that took 2 milliseconds to operate. These characteristics were similar to those of the power conditioning of SERT II. The SERT II thrusters are believed to have failed because of a grid short circuit (ref. 6). In the experiment reported herein, when a fault occurred, an attempt was made to clear it using a capacitor in parallel with the grids. The capacitor was charged from a 1500-volt supply through a large resistance. In this way, the energy stored in the capacitor bank could vaporize the fault without tripping protective circuits of the power supply.

RESULTS AND DISCUSSION

Grid Damage Effects

Arc energy. - The parameter studied in this test was the energy discharged through the grid arc from the capacitor bank. The range of energy per pulse was from 0.28 to 36 joules.

For comparison with later figures, a photomicrograph of a clean, undamaged grid is shown in figure 6. The graininess of the surface should be noted, as it is a property of the undamaged surface and not caused by arcing. Of particular interest are the straight, even edges of the holes, which as will be shown later, are subject to the most serious damage.

The photomicrographs of the typical damage done to the grids are shown in figures 7 to 14 along with the oscillographs of the pulses causing the damage. No detailed discussion of these figures is included herein, and examination of the photographs is left to the reader. In most cases, only the positive grid is shown, since the negative grids were damaged less severely than the positive grids. The value of the energy level, capacitance, and voltage used to cause the damage in each case is given in each figure legend. At all energy levels there was a polishing effect due to surface melting at the spots where the arc occurred. Inside the shiny melted area, at the edges of the holes in the grid, the metal formed long, uneven, ridgelike protrusions (see, e.g., fig. 10(a)).

Another significant form of damage was noticed in the 3-kilovolt, 1-microfarad tests where a small pointed spike extended out about 0.04 millimeter from the side of a web as shown in figure 10(c). In the 2-microfarad, 1.5-kilovolt case (fig. 11) crater-like rings were formed on the molten section of the surface. Spikes about 0.04 millimeter long were also observed.

In the 8-microfarad tests (fig. 12) numerous spikes formed on the edges of the holes in all the tests, the longest being about 0.033 millimeter.

Grid chipping. - In a preliminary test, an unexpected phenomenon was observed. In a test using a 0.25-microfarad capacitor at 1000 volts, where the initial positive pulse duration was relatively short (<0.3 μsec), the grids exhibited a tendency to chip as well as to form polished melted spots on their surface (fig. 14). This chipping was observed only on the grids that were arced no more than three times. The same type of grid allowed to arc 20 times with the same initial conditions showed no chipping effect. Instead, only the previously mentioned surface polishing effects were observed.

It is possible that the chipping occurred only with the first few arcs and that the additional arcs polished the surface and obscured the holes left by the chips. Very few chipped areas exhibited a polished surface. The largest dimension of a chip, judging from the hole left by it, was about 0.27 millimeter. It was observed that a chip could be removed by a single pulse (fig. 15).

Besides damaging the grids, these chips could aggravate the problem of flakes and chips of sputtered conductive material, which cause shorting between thruster grids. From this test, it is seen that some damage occurred at all the energy levels tested.

Grid geometry. - The tests were performed on grid geometry types 1, 2, and 3. Oscillographs of the current pulses through each of the three types of grid material are shown in figure 16. The same apparatus and initial conditions of capacitance, voltage, and energy level (9 J) were used for all three cases. The current pulses varied slightly among the three types of material, which variation indicates some depedence of arc characteristics on the grid structure used. All waveforms shown were found to be repeatable.

The typical damage done to materials of types 1, 2, and 3 is shown in figures 17 to 19. The results show that grid type 1 undergoes far less serious damage for discharges of fixed energy level than either types 2 or 3. The damage sustained by grid types 2 and 3 was very nearly the same: The material had been eroded to a depth of approximately 20 percent of the thickness of the grid. In all cases small spikes formed on the edges of the holes. On grid types 2 and 3 the spikes were about 0.05 millimeter long.

Other protrusions were formed on types 2 and 3 by material that seemed to be "peeled back" from the center of the damage. These protrusions extended about 0.01 millimeter on each side of the web. The smaller damage sustained by grid type 1 is probably due to the better heat-conducting characteristics of the lower open area, thicker webbed material.

Arc duration. - Tests were made to determine the effects of arc duration on grid damage. For an initial energy level of 1 joule, the results of a long and short arc are shown in figures 20 and 21. At a given energy level, a longer lasting arc at a lower voltage is much more damaging than a faster, higher voltage arc (see figs.). The fast arc ($\simeq$1 μsec) did little more than polish the surface; the slower arc ($\simeq$30 μsec) eroded much of the surface and caused 0.051 millimeter spikes to form. These observations, together with those of the previous tests, indicate that for clearing faults (i.e., clearing out small pieces of sputtered materials and surface irregularities causing arcs), a high-voltage, low-capacitance discharge would be more desirable than a low-voltage, high-capacitance discharge.

Arc Characteristics

Arc environment. - The parameter studied in this test was the environment surrounding the grid. In one case the environment was mercury vapor near 1.33×10^{-4} new-

tons per square meter; in the other it was air at atmospheric pressure. The current waveform of an arc occurring in mercury vapor at a measured pressure of 0.439×10^{-4} newtons per square meter is shown in figure 22. The current waveform of an arc sustained by the same apparatus in atmospheric conditions is shown in figure 23. The four parts of each figure are oscillographs taken at increasing sweep rates. The waveforms of both cases are very nearly the same in amplitude as well as frequency. To aid in the interpretation of the oscillographs, it should be noted that the current waveform comprised two parts. The first part was $1\frac{1}{2}$ cycles of a sine wave lasting about 10 microseconds and having a maximum amplitude of several thousand amperes (figs. 22(d) and 23(d)). The second part was an exponential rise starting at -140 amperes and lasting about 3 milliseconds (figs. 22(a) and 23(a)). The damage sustained by the grids at about 1.33×10^{-4} newton per square meter of mercury vapor is presented in figure 24(a). The damage done to the same type of grid material on the same apparatus at atmospheric conditions is shown in figure 24(b). The damage was nearly the same for both cases, but perhaps slightly worse in the mercury vapor case. This may be due to the fact that the arcs all occurred in one spot in the mercury vapor test, while in the atmospheric test the arcs occurred in two different locations.

It is inferred from these results that arcs occurring in the atmosphere closely approximate thruster arcing. Therefore, the experimental data taken at atmospheric conditions provides results that are applicable to the actual conditions in an operating thruster.

Reproducibility. - This test was conducted to see if the current waveform of an arc on a given set of grids change within 20 consecutive arcs. Oscillographs of the 1st, 10th, and 20th waveforms were produced and showed identical waveforms. Since the waveforms are identical, any differences observed in the current waveforms of an arc on one set of grids within at least 20 arcs is due to the change in some factor other than the surface condition of a given set of grids.

Arc simulation. - To establish the validity of the seemingly large values of current recorded on the oscillographs of this study, an analog computer simulation was run with the arc represented as a short circuit. In figure 25(a) the oscillograph of the current pulse through a set of grids is shown. The analog simulation of a similar current pulse is shown in figure 25(b). The plots do not compare exactly, as the experimental circuit-element values result from the distributed impedances in a typical grid arc setup, exclusive of the source capacitor and the simulation of figure 25(b) used slightly larger values for these parameters. The analog simulation did verify the high-current values recorded. A rigorous analog simulation of the experimental arc obviously exists for some combination of R, L, and C between those used to obtain the transients of figures 25.

Arc attenuation. - The 1500-ampere current pulse of figure 25(a) was experimentally decreased to a few amperes by using various inductances and resistances as ballasts.

However, the arc duration was increased from about 8 microseconds in the unballasted case to about 7 milliseconds in the ballasted cases.

The 60-millihenry, 245-ohm choke attenuated the peak arc current to about 2.7 amperes (fig. 26). A 250-ohm noninductive resistor similarly attenuated the current, but the amplitude of its current pulse was 25 percent higher than that of the pulse through the choke (fig. 27). The choke also rounded the peak of the pulse and increased its rise-time. The 60-millihenry, 245-ohm air core case also matched closely with its analog computer simulation (fig. 28). A few hand calculated values to check the computer plot are included in figure 29 (see appendix). A few points from the oscillograph of figure 26 are also plotted on the curve. All three sets of values agree reasonably well.

The current pulse through the 5-henry, 300-ohm choke (fig. 28) did not agree with the analytical results. Because the choke had an iron core and was rated for a maximum of 100 milliamperes, the 2-ampere pulse saturated its core, thus changing its characteristics considerably. This case was tested, however, because a similar choke had been used in a thruster test to eliminate neutralizer quenching during grid arcs (ref. 5). The analog computer simulation of this case is shown in figure 30 along with a few hand calculated points serving as a check on the simulation. Although the hand calculation and the analog simulation agree favorably, in practice, the theoretical transient current is never realized because of saturation effects.

As shown by the oscillographs of figures 27 and 31, a ballast resistor may be adequate for limiting the amplitude of the arc. The net effects of a slower current rise and attenuation of the higher frequency components of the arc transient particularly with regard to neutralizer stability are not known at this time. As shown in figure 32, grid damage occurs even with the arc current attenuated to a 3-ampere level. The damage was due to an arc from an 8 microfarad capacitor charged to 1000 volts and ballasted by a 250-ohm resistor. Although the amplitude of the current pulse was low, the duration of the pulse (3 μsec) was much longer than that of the pulse in the unattenuated case (8 μsec). The damage observed here is much less, however, than that occurring in the 1.5-kilovolt, 8-microfarad, unballasted case (fig. 18). In view of the information available at this time, a simple ballast resistor used in series with the grids is an effective means of attenuating the arc current and the resulting grid damage.

Chip Clearing Test

Causing faults. - When a chip was dropped between the grids, a short occurred. The chip would sometimes weld in place forming a smooth spike on the positive grid, and the overcurrent protection would shut off the power supply (see fig. 33). Most of the faults caused in this manner would be vaporized by the current surge that turned

off the power supply, and the supply would reset without additional arcing. However, a small percentage of the fault causing chips would cause a permanent fault that would prevent the supply from resetting. About 100 single chips had to be dropped between a set of grids until a permanent fault occurred. A fault was considered permanent if it did not vaporize after the power supply had been tripped 30 times. The power supply was tripped as many as 100 times by a single fault. A pure short caused by metallic contact between both grids (a chip) was observed only once during the tests. In this particular case, a chip landed on the top grid and stopped. When another chip was dropped through the grids it simultaneously tripped the power supply and caused the other chip to become lodged between the grids while the power supply was off. The power supply would not reset. The chip was removed using a 0.5 microfarad capacitor charged to 1500 volts. The capacitor was discharged through the grids, vaporizing the chip, with no significant grid damage.

Clearing faulted grids. - Grids were cleared using the arrangement shown in figure 34. A capacitor was charged from a 1500-volt supply through a large resistance until the breakdown potential was reached. In this manner, the energy from the capacitor bank would cause an arc to occur without tripping the supply. The capacitor would then recharge until another arc occurred. This breakdown would repeat until the fault was cleared. A large resistance of 2×10^7 ohms and a small capacitance of 0.02 microfarad were effective in clearing faults without serious grid damage. The charge-discharge cycle would repeat itself for a few seconds until the fault was gone. A smaller resistance of 470 kilohms was used with the 0.02 microfarad capacitor, but the charging time was insufficient to permit the grid surface to transfer the heat away between arcs, and serious grid damage resulted. Larger charging time constants were obtained using capacitances of 0.5, 8.0, and 10.0 microfarads with a 470 000-ohm resistor. Fault clearing with these component values resulted in no serious grid damage, but the results of the arc duration test indicate that the longer lasting arcs produced by larger values of capacitance are potentially damaging to grids. Figure 35 shows the surface of a positive screen grid after removal of a fault. An attractive flight technique for removal of grid shorting chips would be a switching system which would charge a properly-sized capacitor and then switch it in to the shorted screen-accelerator grid circuit, vaporizing the chip.

CONCLUSIONS

Arcs occurring between mercury ion thrusters grids were simulated and studied. Damage resulting from such arcs was related to power conditioning and grid geometries by varying arc energy and duration and grid geometry. Attenuation of arc damage was

also studied. Potentially serious grid damage occurred at all energy levels representative of actual thruster operating conditions. Thinner webbed, high open area grids were damaged far more severely than the thicker webbed, low open area, grids. Most of the damage observed was due to melting of the grid surfaces and the resulting distortion of these molten surfaces. At a fixed energy level, longer duration, lower voltage arcs were more damaging than short duration, high voltage arcs. This information should be helpful in developing future methods of clearing grids, which are faulted by chips of sputtered material during thruster operation. These principles have already been applied successfully to clearing grid-to-grid shorts in recent thruster life tests (ref. 7).

Ballasts and chokes greatly reduced the current amplitude and resulting damage of the arc but at the same time increased the time duration of the arc.

Lewis Research Center,
National Aeronautics and Space Administration,
Cleveland, Ohio, January 11, 1974,
502-04.

APPENDIX - MATHEMATICAL VERIFICATION OF OSCILLOGRAPHS

A mathematical analysis of the arc circuit, done to verify the accuracy of the oscillographs, is presented in this appendix. Since the arc involved was nearly instantaneous with very high currents, it was represented as a direct short. On this basis the following analysis was performed.

The Q of a typical circuit (including busbars) was measured and used to obtain the parameters necessary for an analog computer simulation and for hand calculations. In this case, the circuit parameters were as follows:

Capacitance, C, μF	0.46
Circuit, Q, dimensionless	8.84
Frequency, ω, rad/sec	2.38×10^{6}
Inductance, L, H	0.385×10^{-6}
Damping ratio, ξ, dimensionless	0.13
Resistance, R, ohm	0.234
Initial voltage, V_0, kV	1.5

For the hand calculations these parameters are used in the relation for the underdamped oscillatory case (see ref. 4)

$$i(t) = \frac{V_o}{\omega_o L \sqrt{1 - \xi^2}} e^{-\xi \omega_o t} \sin\left(\omega_o \sqrt{1 - \xi^2}\, t\right)$$

where i(t) peak was determined by setting the first derivative of i(t) equal to zero, solving for the time and substituting it back in the original equation. It was found that

$$t_{i_{peak}} = 0.61\times10^{-6} \text{ sec}$$

$$i_{peak} = 1350 \text{ A}$$

These values agree with the oscillograph of this case in figure 36. The computer simulation of this case is presented in figure 36(b). A similar method was used in the case of figure 29 with good results. A check on the computer plot of figure 29 was made using the relation (see ref. 4)

$$i(t) = e^{-\xi \omega_o t}\left(k_1 e^{\omega_o \sqrt{\xi^2-1}\, t} + k_2 e^{-\omega_o \sqrt{\xi^2-1}\, t}\right)$$

Using the initial conditions, it can be shown that $K_2 = -K_1$. Taking the first derivative of i(t) and using the relation (see ref. 4), it was found that $K_1 = 5.95$. Thus, the equation can be used to obtain the points shown in figure 29. Data are also shown plotted from the oscillograph of an arc occurring in a circuit with these parameters. The oscillograph from which those points were taken is shown in figure 27.

REFERENCES

1. Free, Bernard; and Huson, George: Selected Comparisons Among Propulsion Systems for Communications Satellites. Paper 72-517, AIAA, April 1972.

2. Hudson, Wayne R.; and Banks, Bruce A.: An 8-cm Electron Bombardment Thruster for Auxiliary Propulsion. NASA TM X-68296, 1973.

3. Kerslake, William R.: Charge-Exchange Effects on the Accelerator Impingement of an Electron-Bombardment Ion Rocket. NASA TN D-1657, 1963.

4. Van Valkenburg, Mac Elwyn: Network Analysis. Prentice Hall, Inc., 1959, pp. 102-111.

5. Nakanishi, S.; and Finke, R. C.: A 2000-Hour Durability Test of a 5-Centimeter Diameter Mercury Bombardment Ion Thruster. NASA TM X-68155, 1972.

6. Bagwell, James W.; Hoffman, Anthony D.; Leser, Robert J.; Reader, Karl F.; Storer, John B.; and Vasicek, Richard W.: Review of Sert II Power Conditioning. NASA TM X-2085, 1971.

7. Nakanishi, S.; and Finke, R. C.: A 9700-Hour Durability Test of a Five Centimeter Diameter Ion Thruster. NASA TM X-68284, 1973.

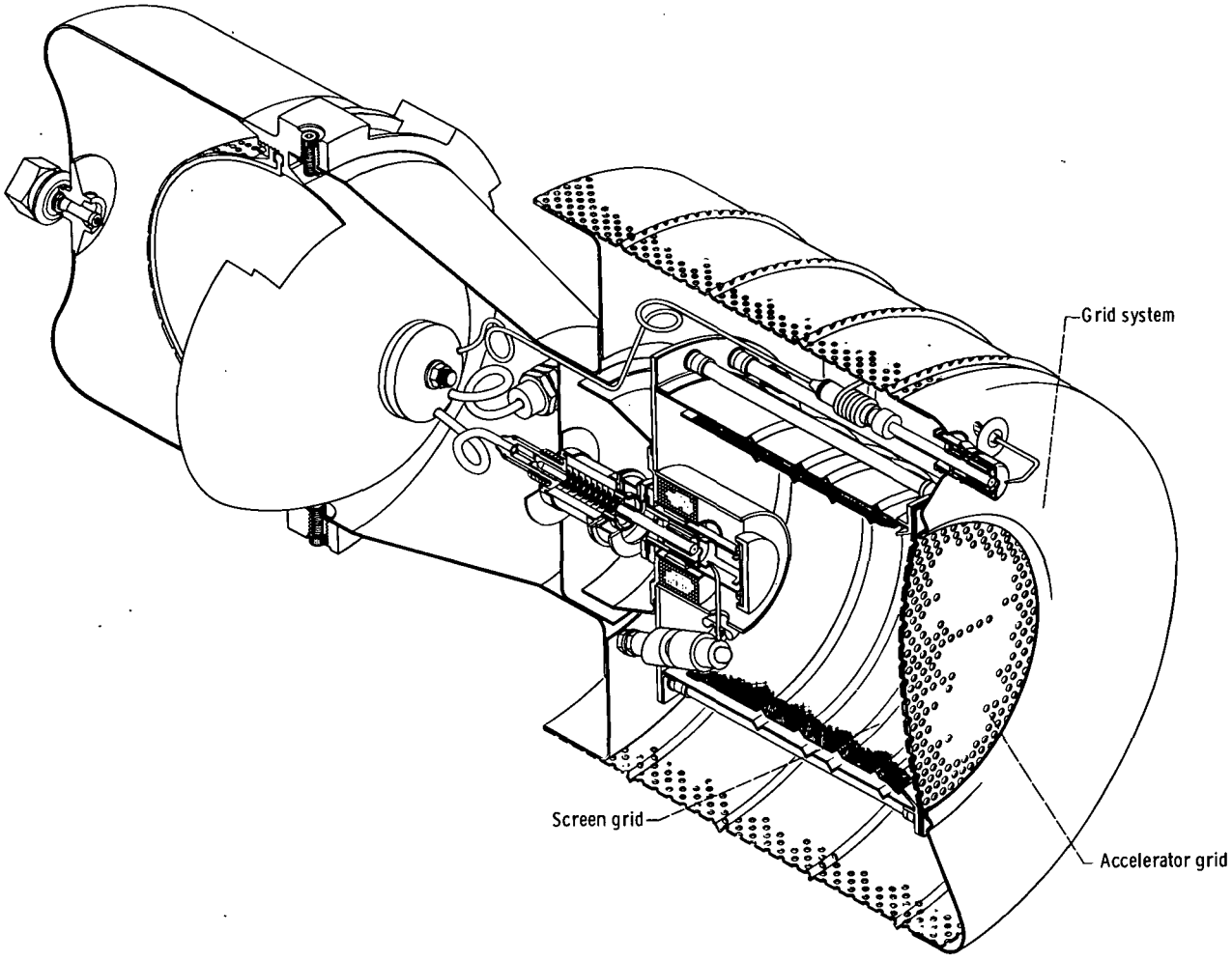

Figure 1. - Sketch of an 8-centimeter mercury bombardment ion thruster showing the grids.

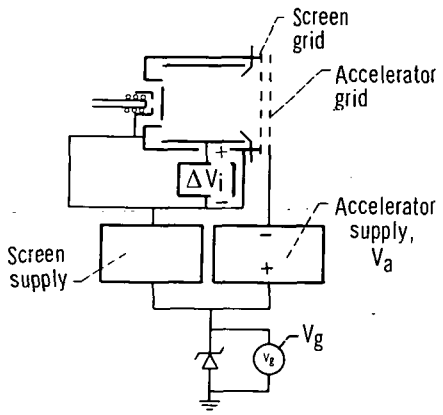

Figure 2. - High-voltage wiring diagram of thruster.

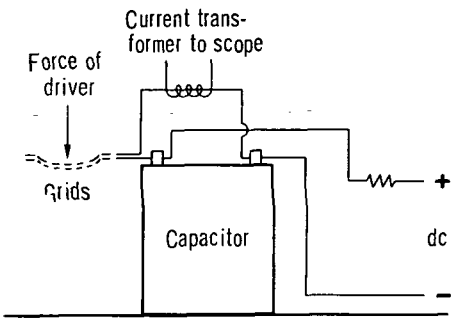

Figure 3. - Apparatus used to discharge an arc between two grids.

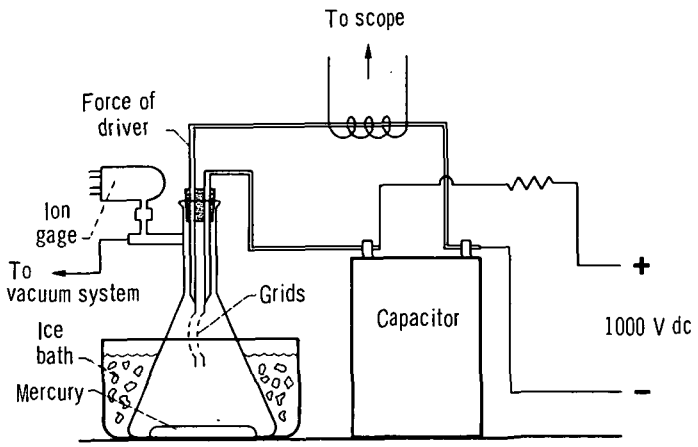

Figure 4. - Apparatus used to simulate ion thruster arc.

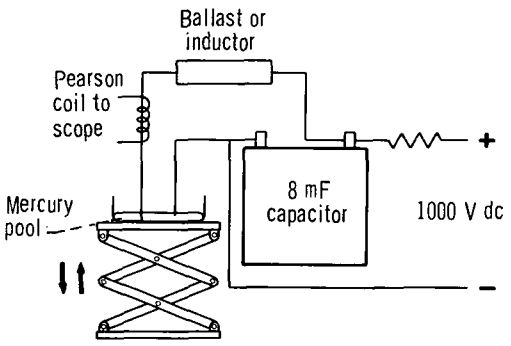

Figure 5. - Apparatus used in arc attenuation tests.

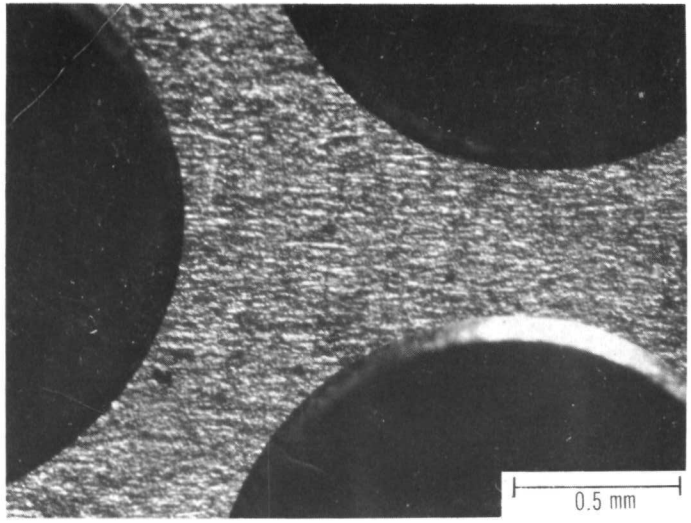

(a) Magnification, X45.

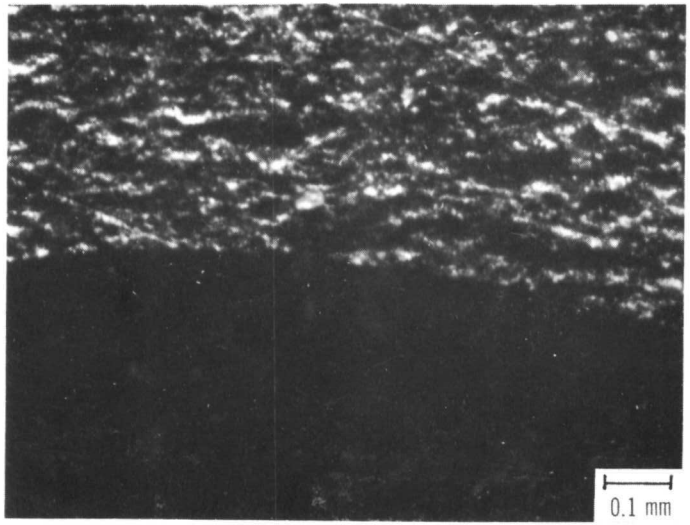

(b) Magnification, X100.

Figure 6. - Clean molybdenum grids.

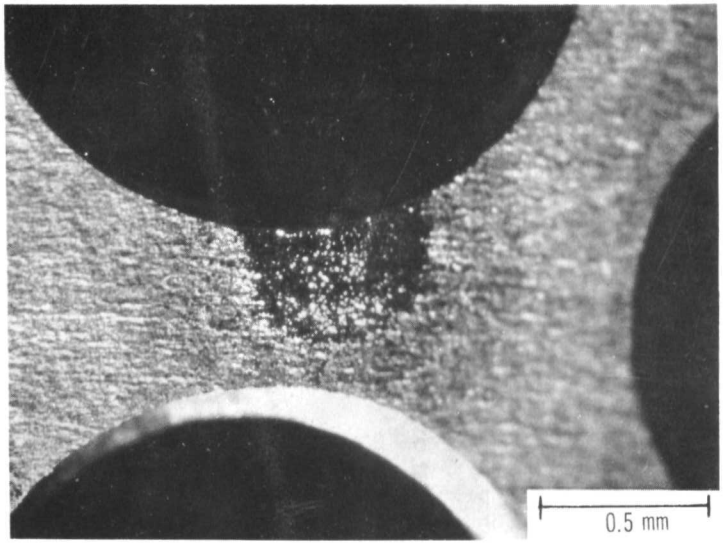

(a) Positive grid.

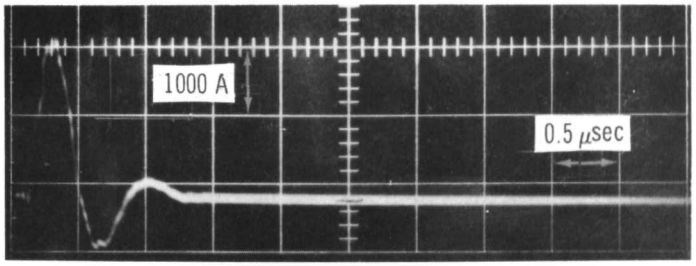

(b) One pulse causing damage.

Figure 7. - Grid damage caused by 1.5 kilovolts, 0.25 microfarad, and 0.281 joule per pulse.

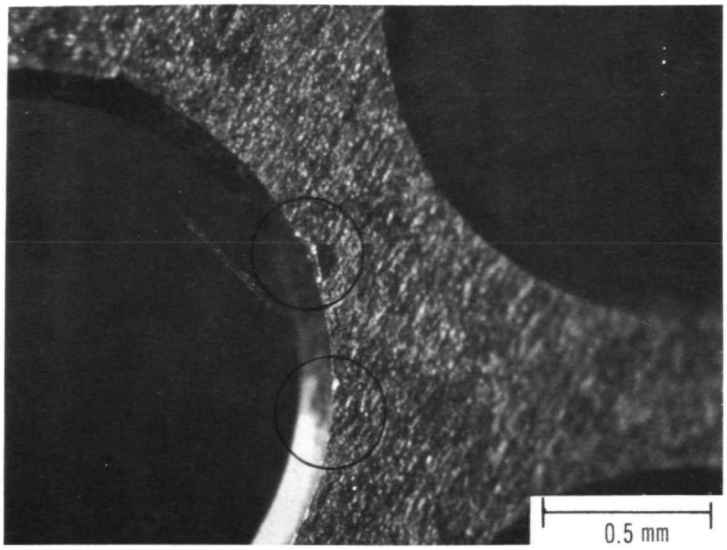

(a) Positive grid.

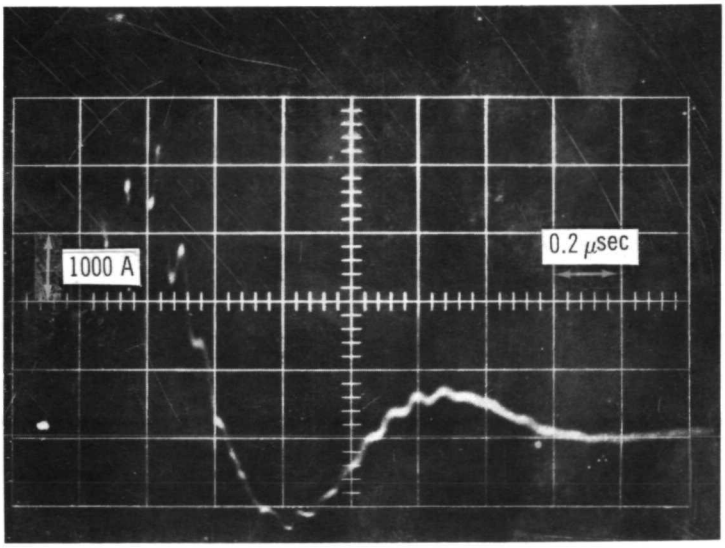

(b) Pulse causing damage.

Figure 8. - Grid damage caused by 0.25 microfarad, 3 kilovolt arcs.

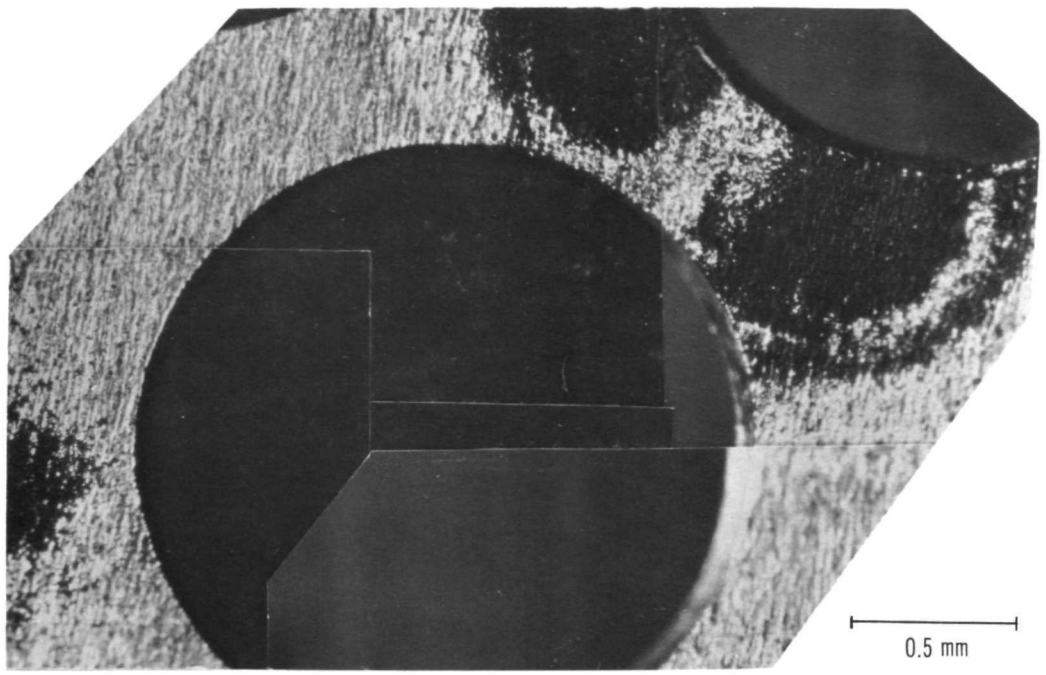

(a) Positive grid.

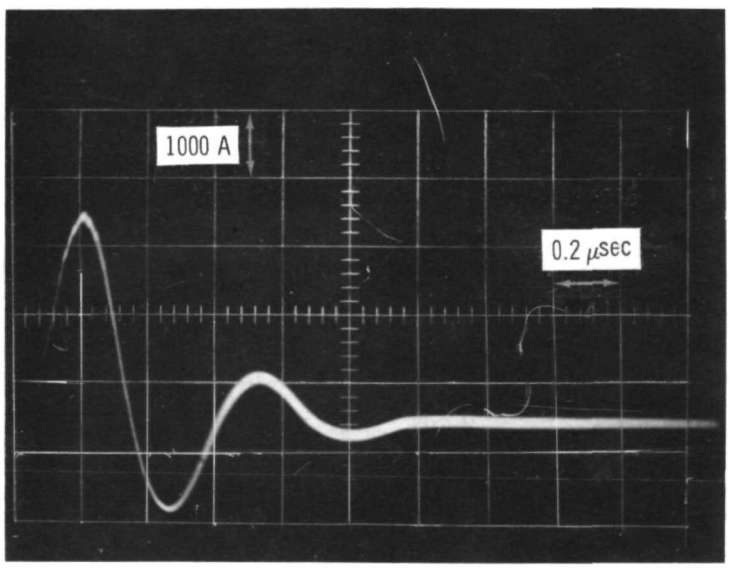

(b) Pulse causing damage.

Figure 9. - Grid damage caused by 1 microfarad, 1.5 kilovolts, and 1.12 joules per pulse.

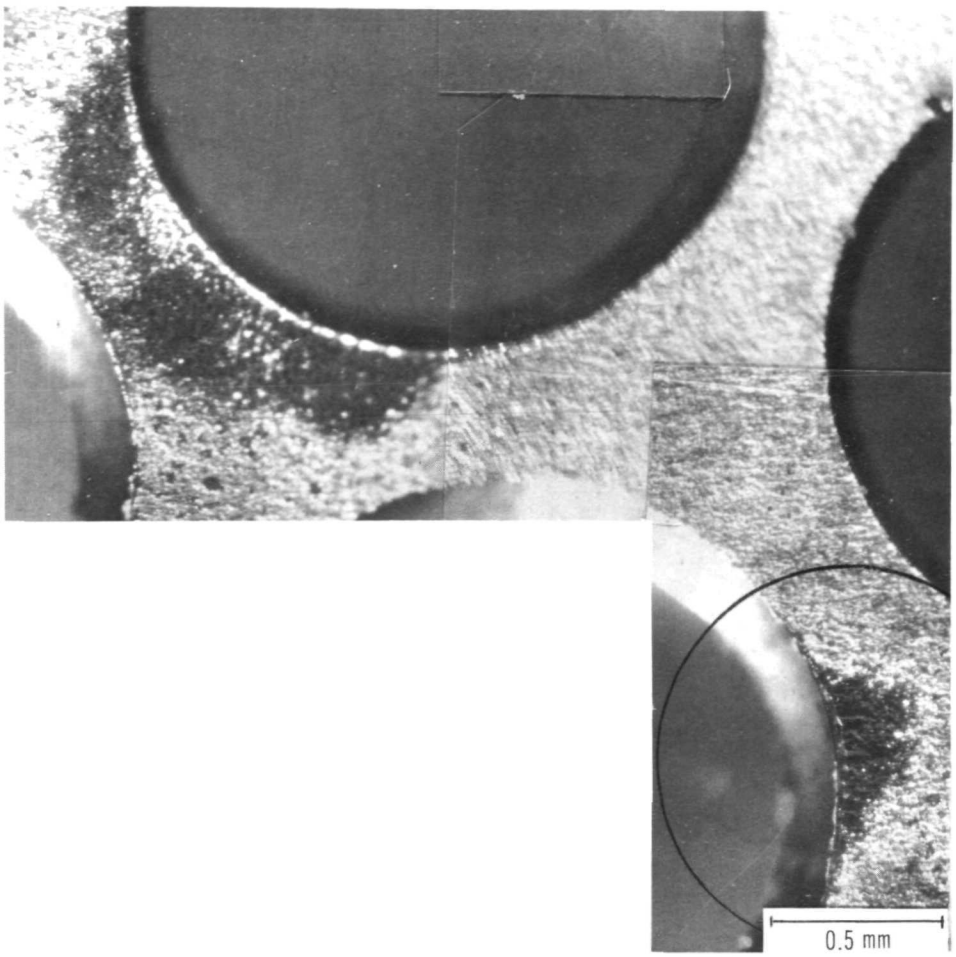

(a) Positive grid.

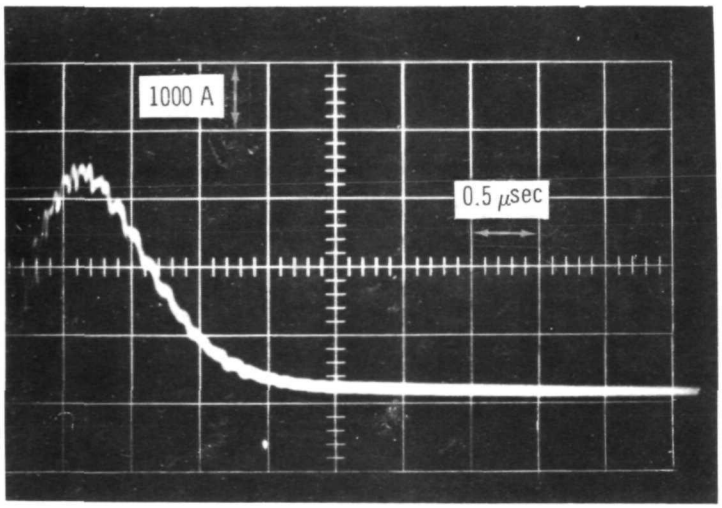

(b) Pulse causing damage.

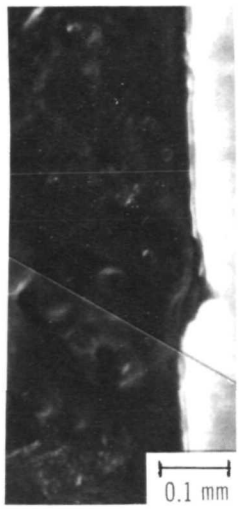

(c) Spike formed on grid.

Figure 10. - Grid damage caused by 1 microfarad, 3 kilovolts, and 4.5 joules per pulse.

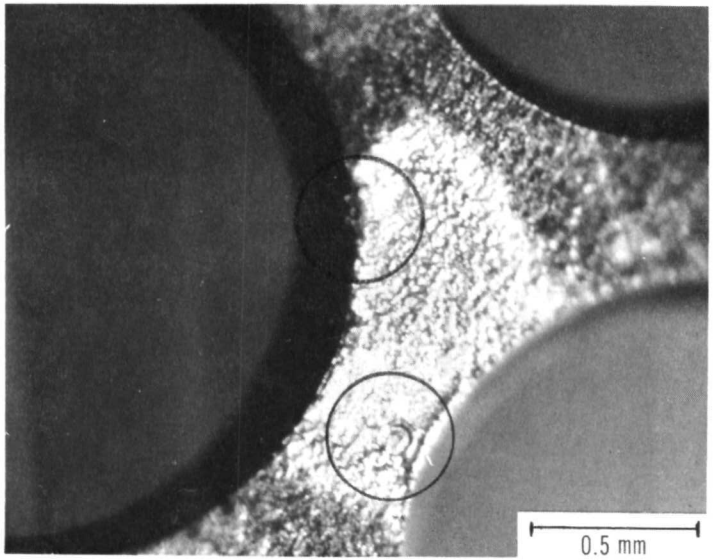

(a) Positive grid.

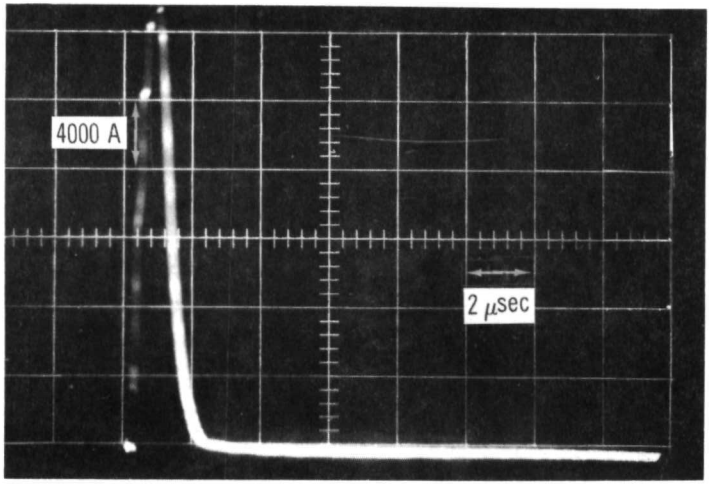

(b) Pulse causing damage.

Figure 11. - Grid damage caused by 2 microfarads, 1.5 kilovolts, and 2.25 joules per pulse.

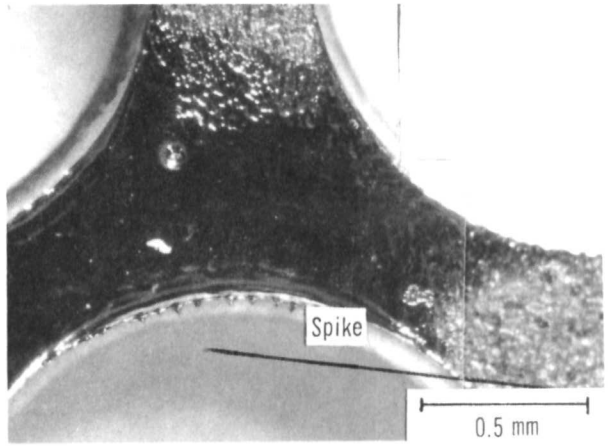

(a) Positive grid. X45.

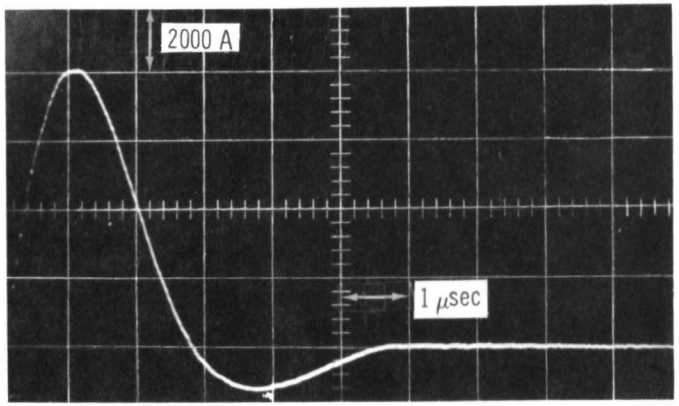

(b) Pulse causing damage.

Figure 12. - Grid damage caused by 8 microfarads, 1.5 kilovolts, and 9 joules per pulse.

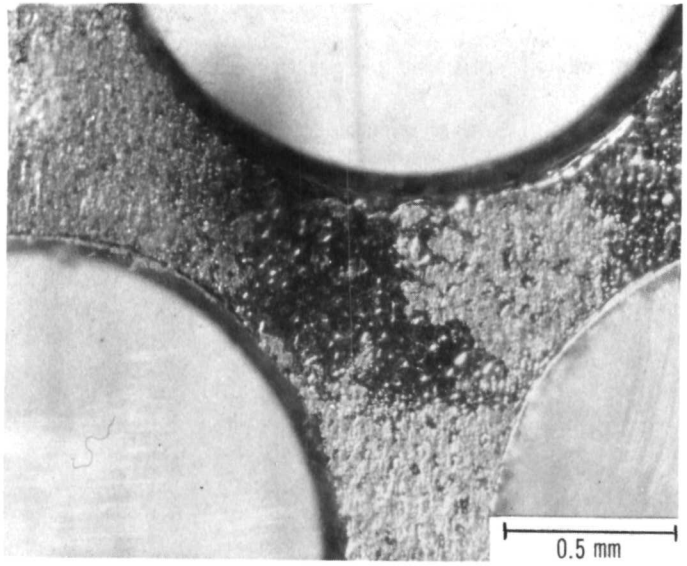

(a) Positive grid.

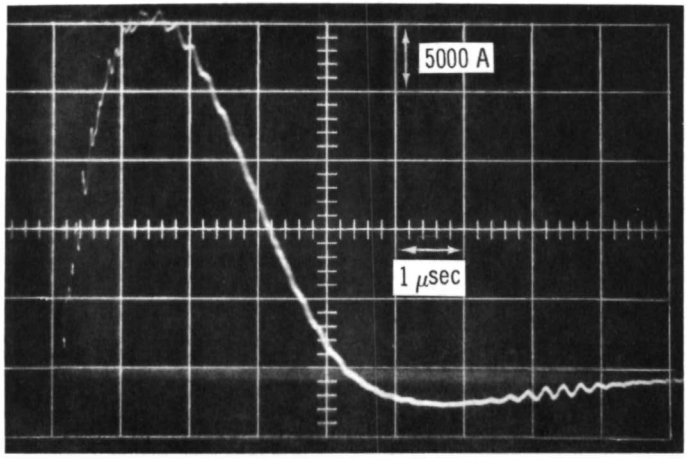

(b) Pulse causing damage.

Figure 13. - Grid damage caused by 8 microfarads, 3 kilovolts, and 36 joules per pulse.

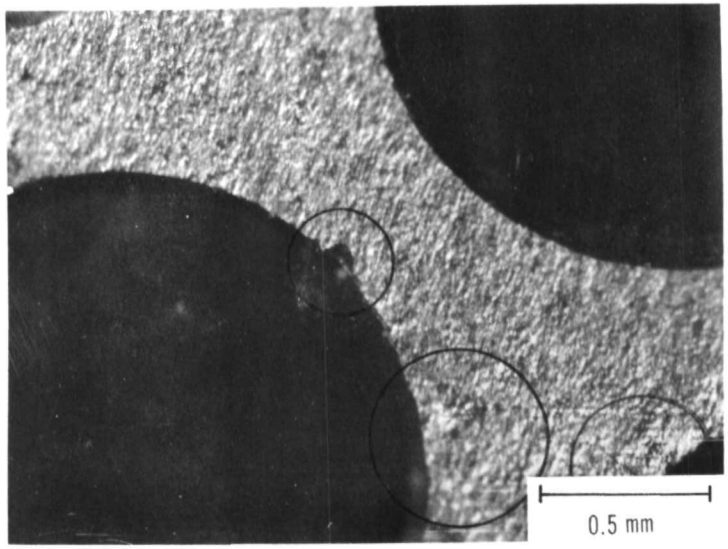

(a) Grid type 1.

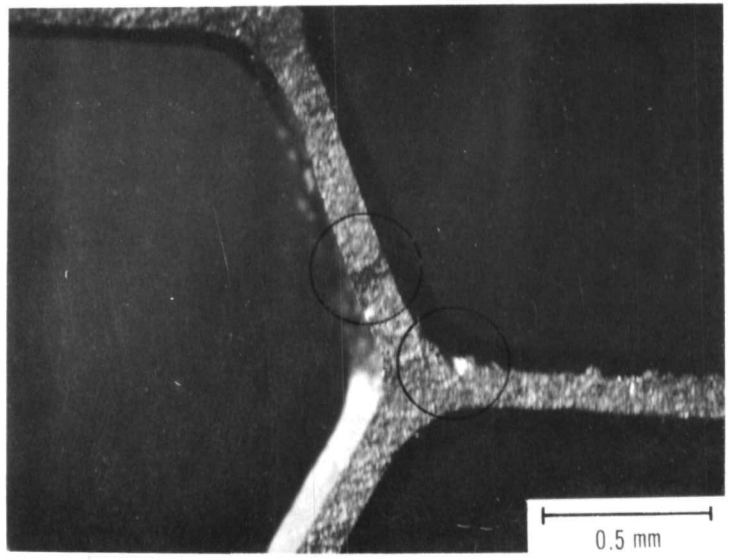

(b) Grid type 2.

Figure 14. - Grid chipping from three pulses.

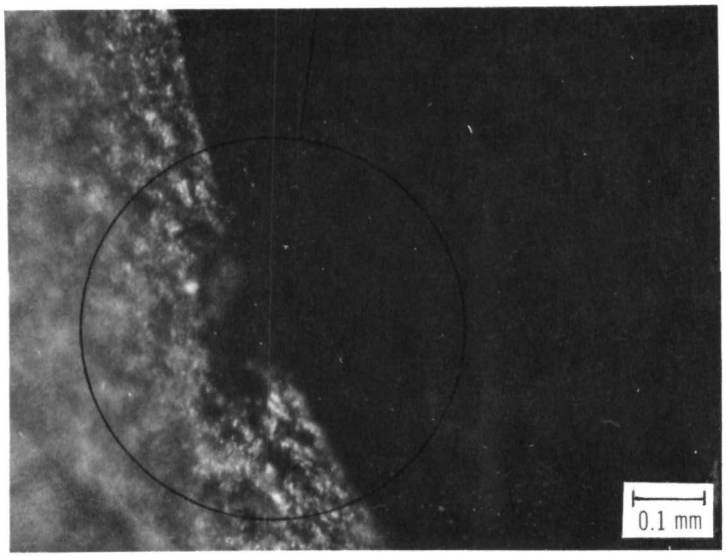

Figure 15. - Grid chipping from one pulse. X100.

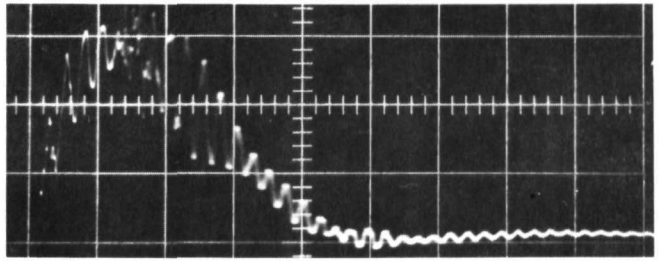

(a) Grid type 1.

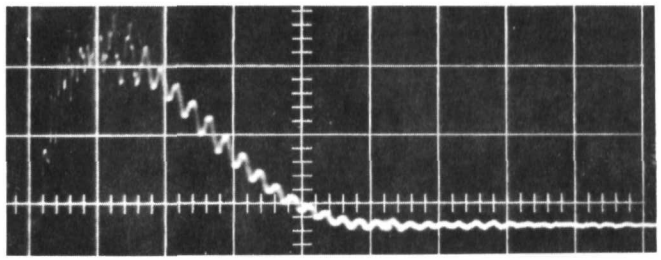

(b) Grid type 2.

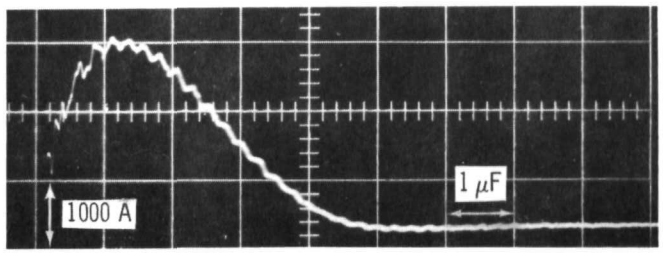

(c) Grid type 3.

Figure 16. - Current pulses discharging from energy banks with identical initial conditions through the three types of grid materials.

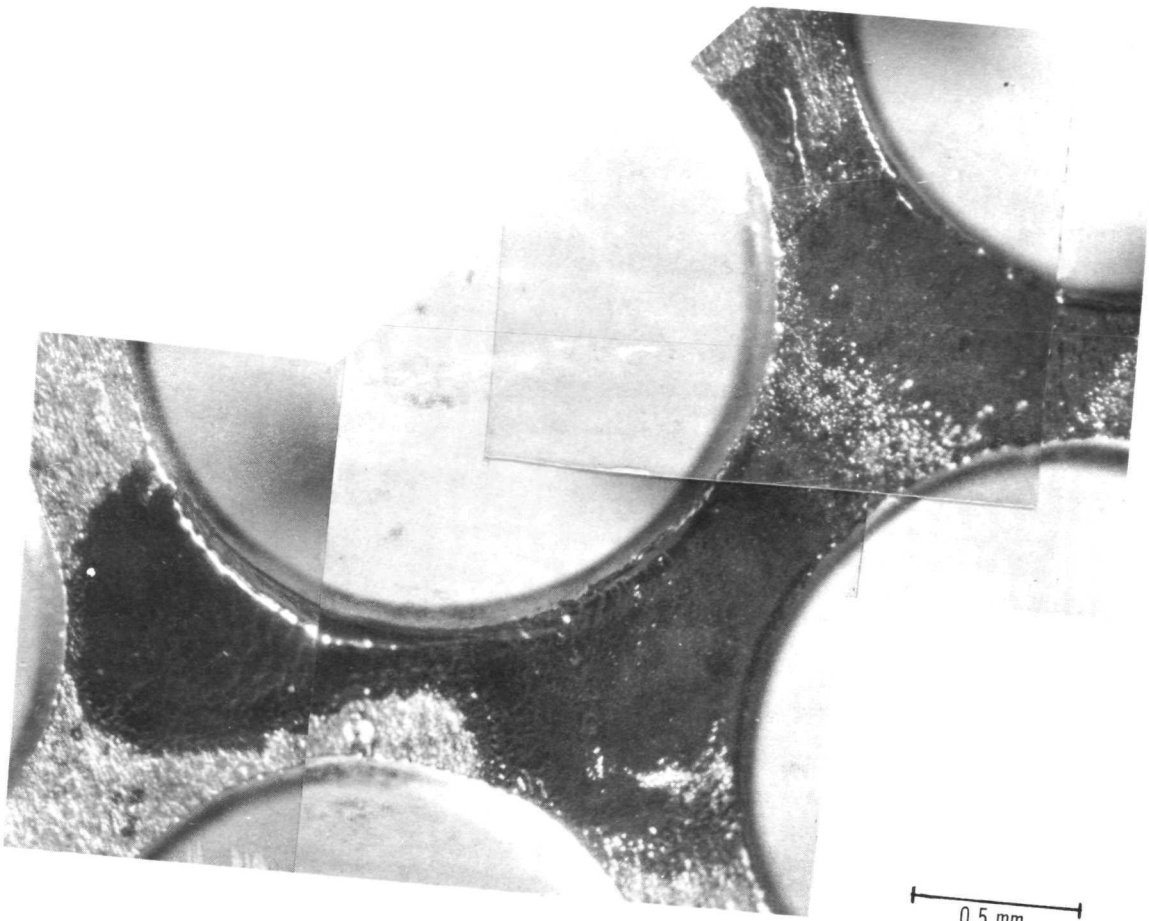

(a) Magnification, X45.

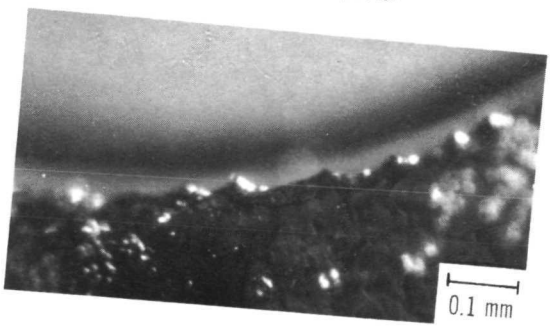

(b) Magnification, X100.

Figure 17. - Grid geometry test damage. Type 1 positive grid. Initial voltage, 1.5 kilovolts, capacitance, 8 microfarads.

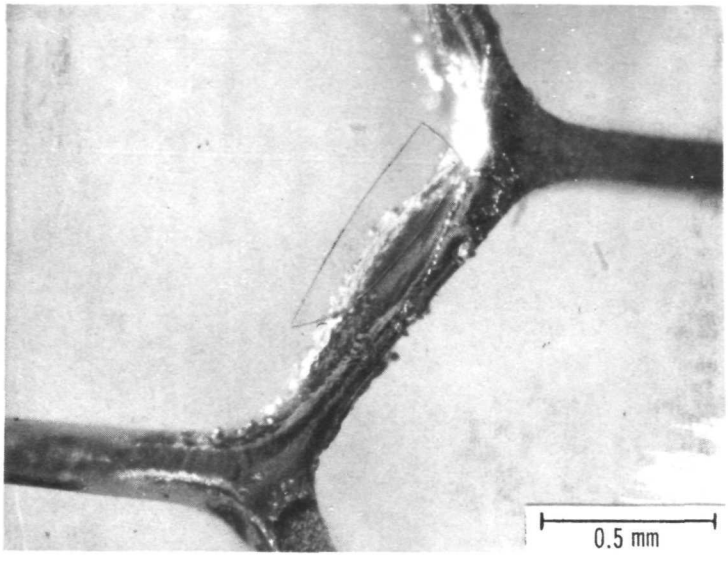

Figure 18. - Grid geometry test damage. Grid type 2 positive grid. Initial voltage, 1.5 kilovolts; capacitance, 8 microfarads.

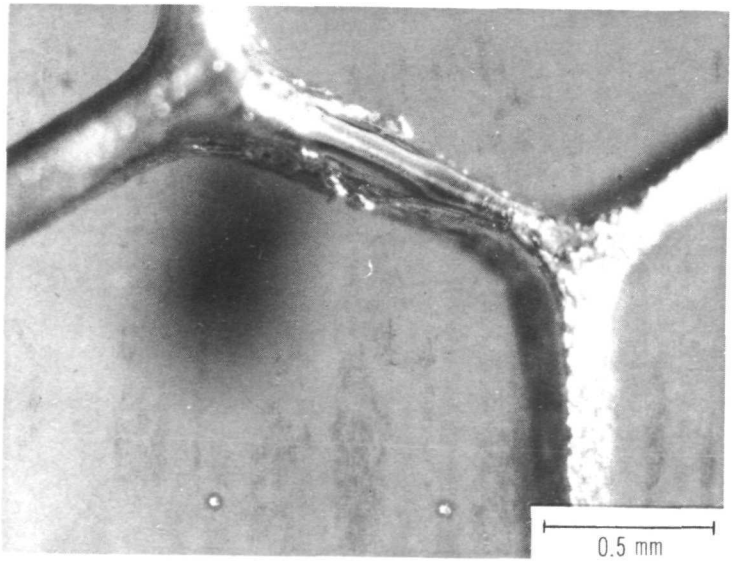

Figure 19. - Grid geometry test damage. Type 3 positive grid. Initial voltage, 1.5 kilovolts; capacitance, 8 microfarads.

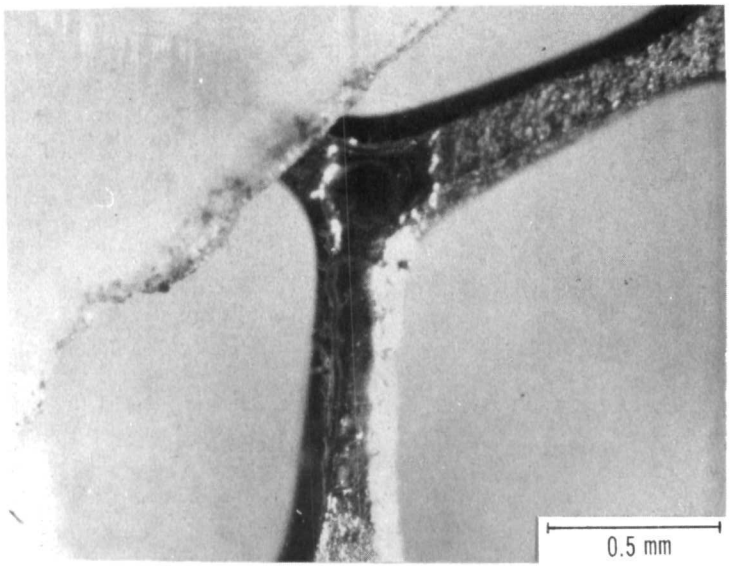

(a) Positive grid damage.

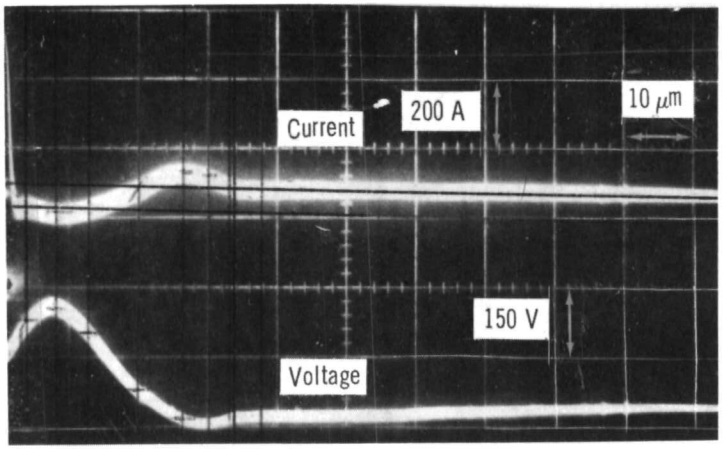

(b) Current and voltage pulses causing damage.

Figure 20. - Arc duration tests; long pulse.

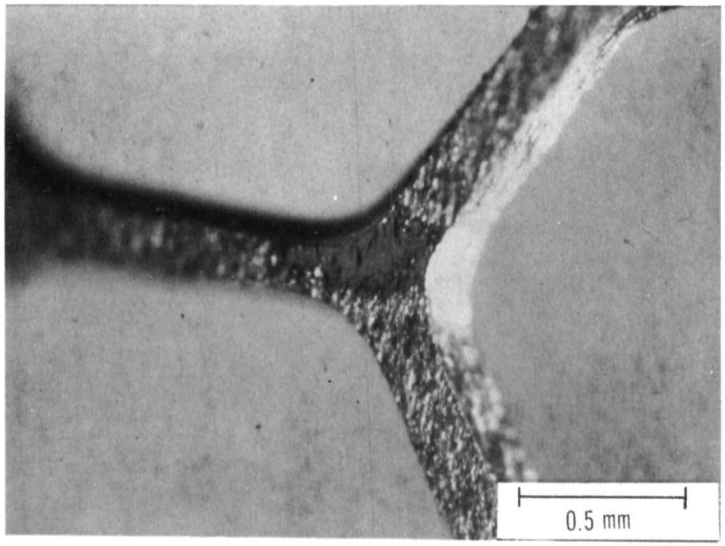

(a) Positive grid damage.

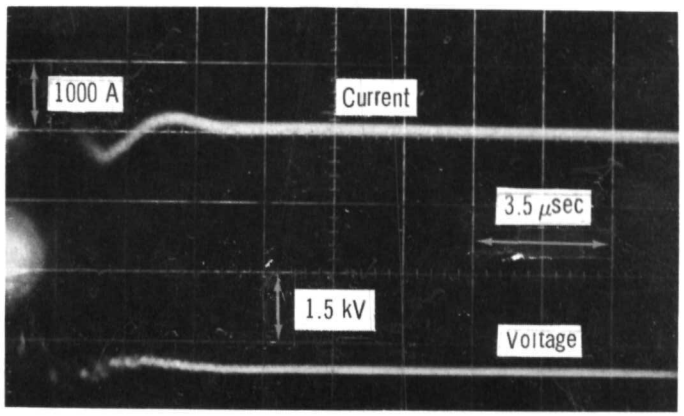

(b) Current and voltage pulses causing damage.

Figure 21. - Arc duration tests; short pulse.

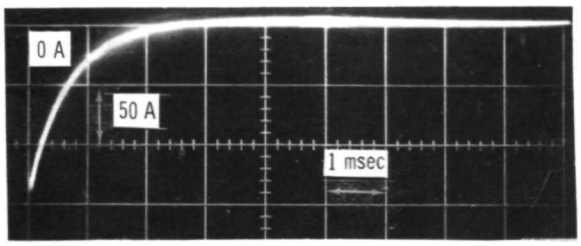

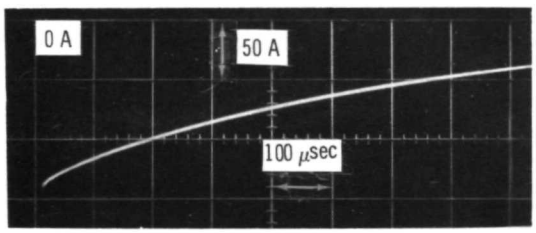

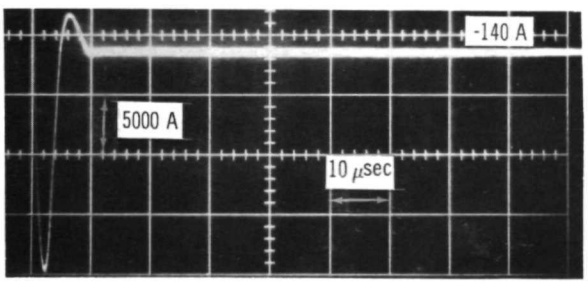

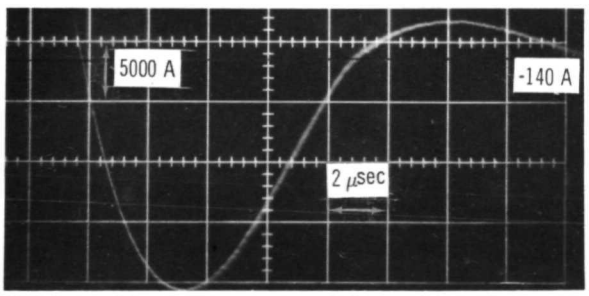

Figure 22. - Simulated thruster arc current pulses occurring in mercury vapor at vapor pressure of $0.33X10^{-4}$ torr.

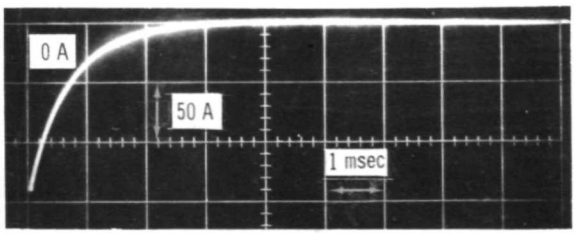

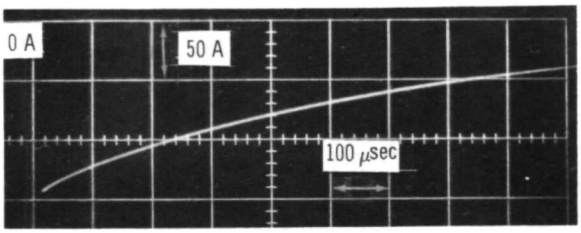

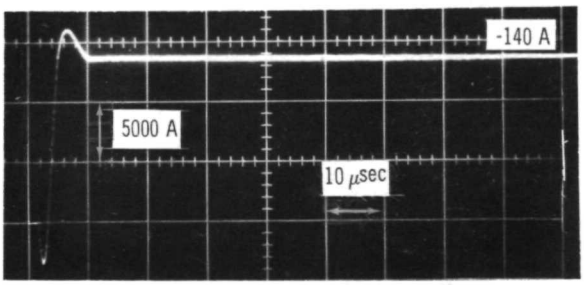

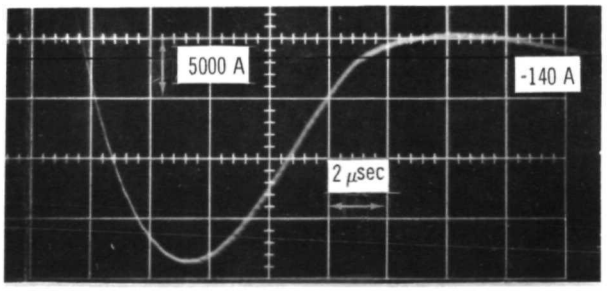

Figure 23. - Simulated thruster arc current pulses at atmospheric pressure.

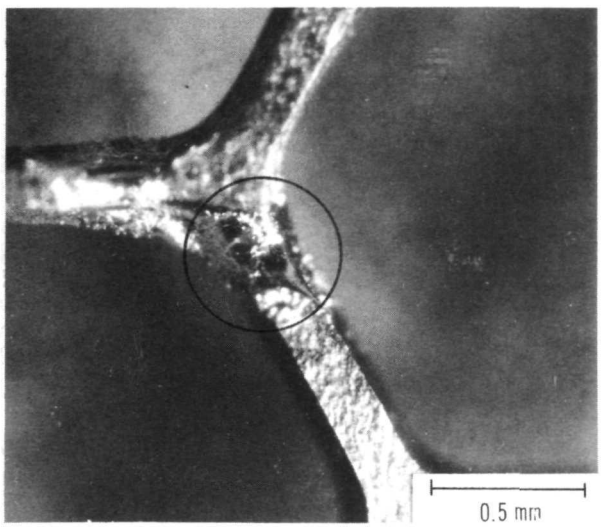

(a) Arc damage with mercury vapor present.

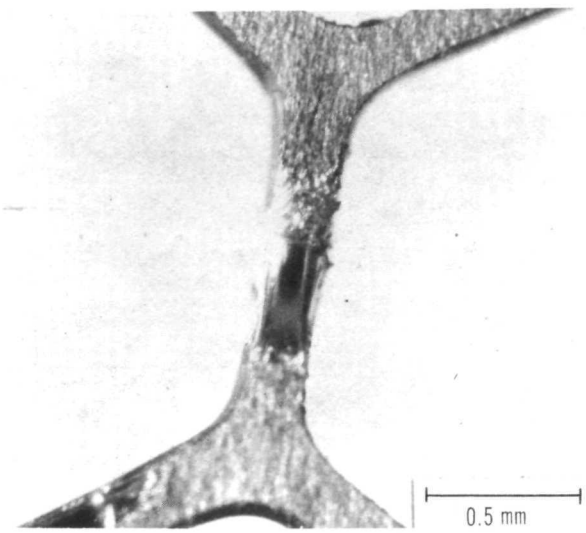

(b) Arc damage occurring at atmospheric pressure.

Figure 24. - Damage resulting from current pulses shown in figures 22 and 23.

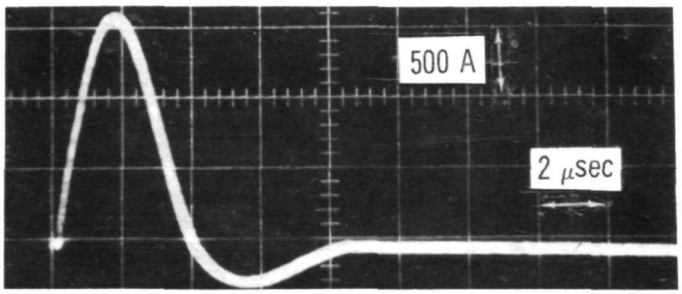

(a) Experimental arc.

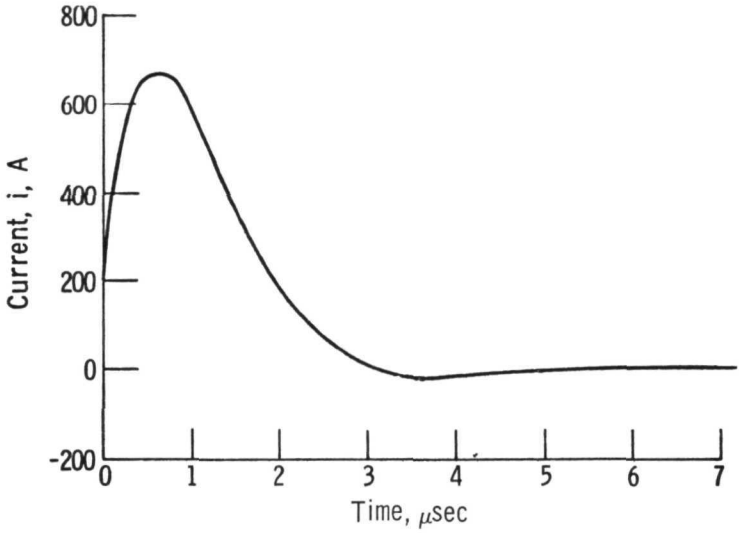

(b) Analog computer plot of RLC circuit. Capacitance, 1 microfarad; inductance, 4 microhenry; resistance, 1 ohm; initial voltage, 1 kilovolt.

Figure 25. - Current waveform of arc with no series impedance.

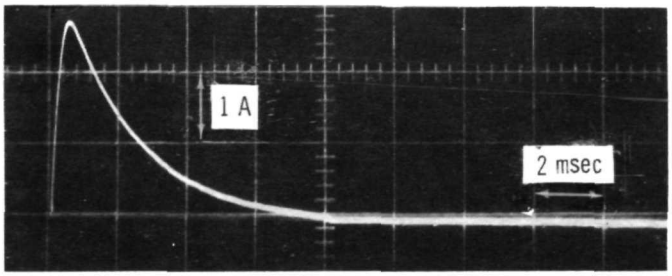

Figure 26. - Arc attenuation test current pulse with 60-millihenry, 245-ohm choke in series.

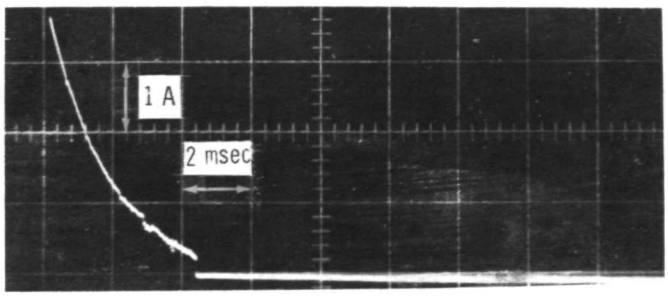

Figure 27. - Arc attenuation test current pulse with 250-ohm, non-inductive resistance in series.

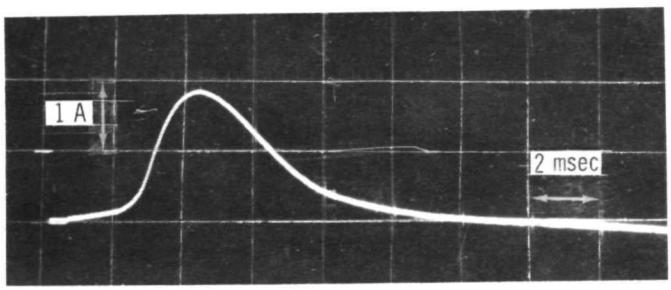

Figure 28. - Arc attenuation test current pulse with 5-henry, 300-ohm choke.

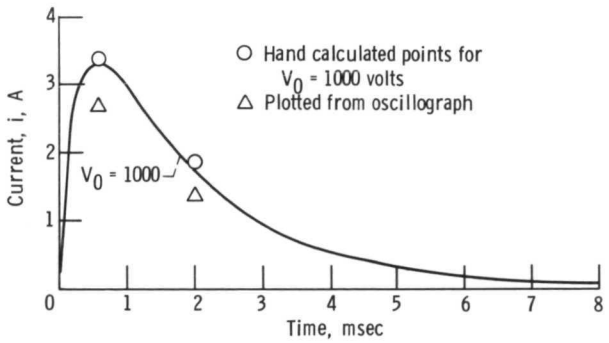

Figure 29. - Analog computer plot of RLC circuit. Capacitance, 8 microfarads; inductancd, 60 microhenries; resistance, 250 ohms; initial voltage, 1 kilovolt.

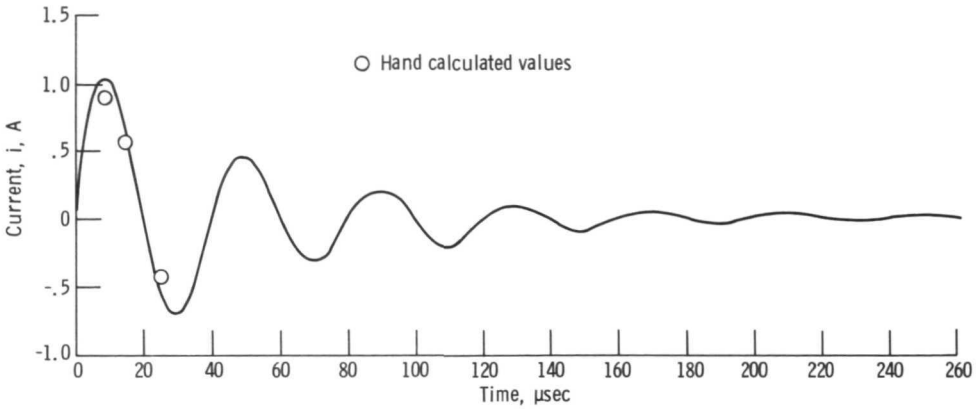

Figure 30. - Analog computer plot of RLC circuit. Capacitance, 8 microfarads; inductance, 5 henries; resistance, 300 ohms; initial voltage, 1 kilovolt.

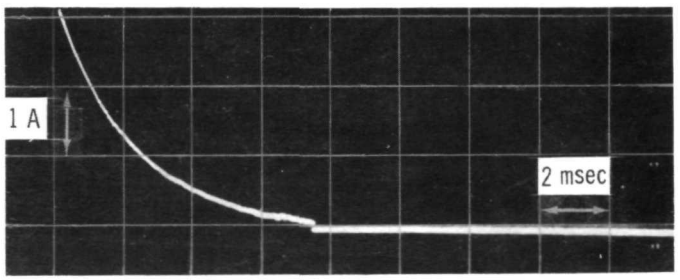

Figure 31. - Arc attenuation test current pulse with 300-ohm non-inductive resistor in series.

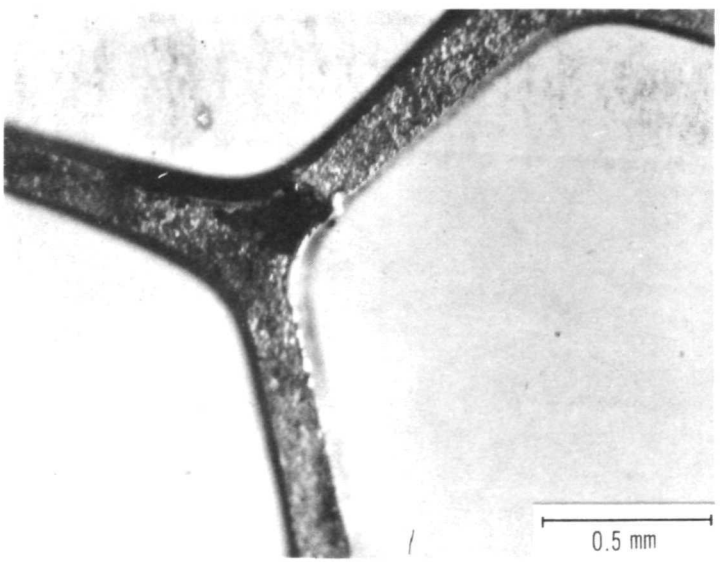

Figure 32. - Arc damage to grid from arc attenuated using 250 ohm non-inductive resistor. Initial voltage, 1 kilovolt; current, 8 microfarads. X45.

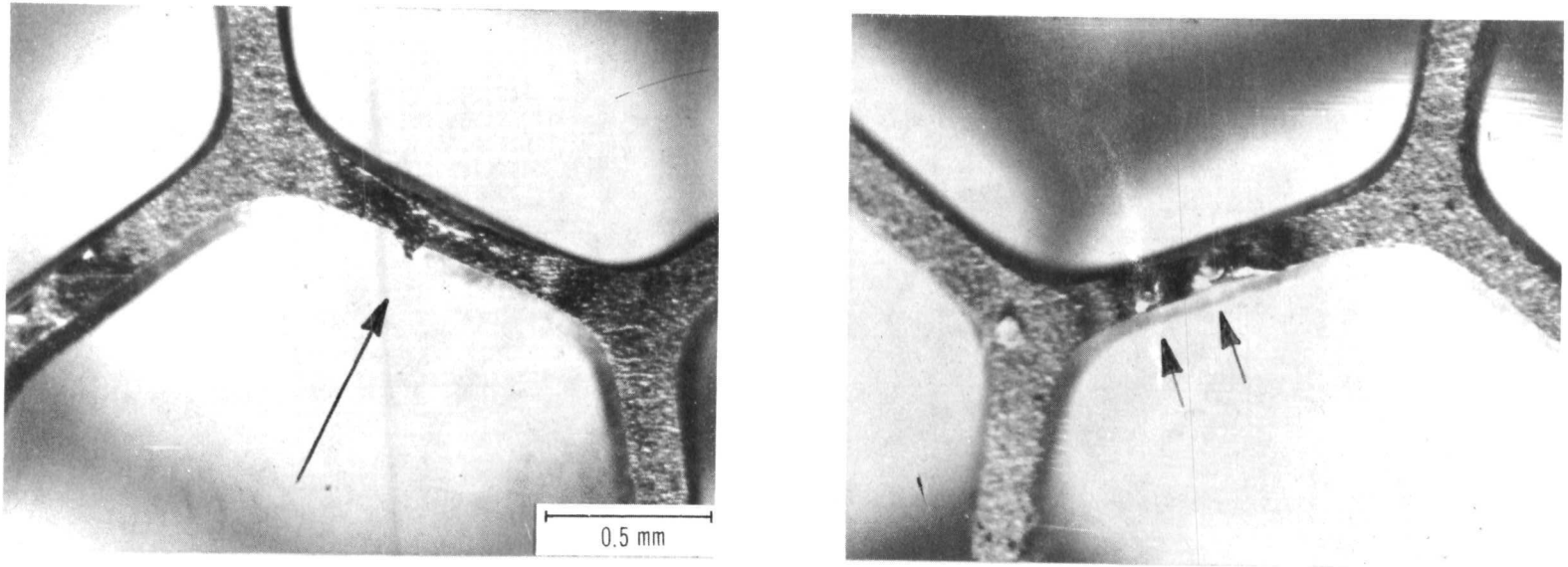

Figure 33. - Metal flakes from inside thruster which have shorted the grids and welded in place to form smooth spikes between the grids.

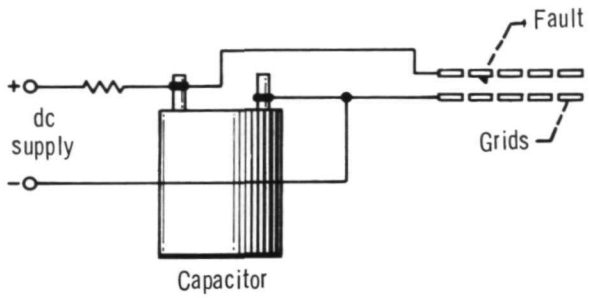

Figure 34. - Apparatus used to clear faulted grids.

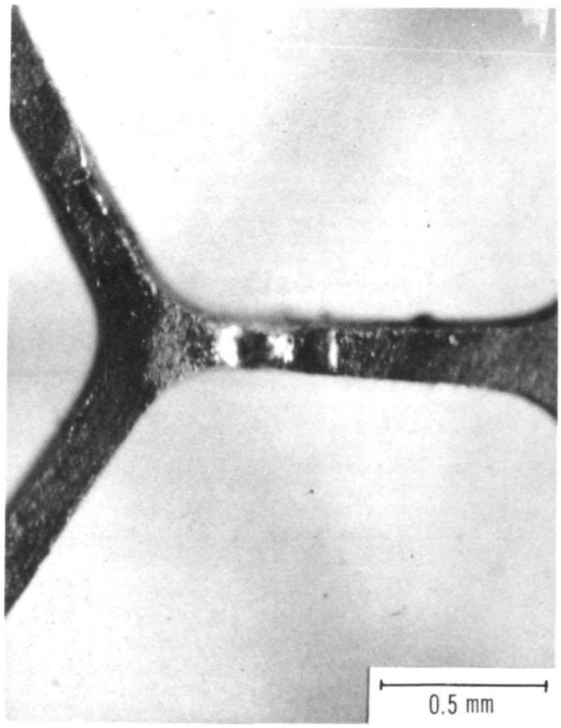

Figure 35. - Grid surface after removal of metallic chip fault.

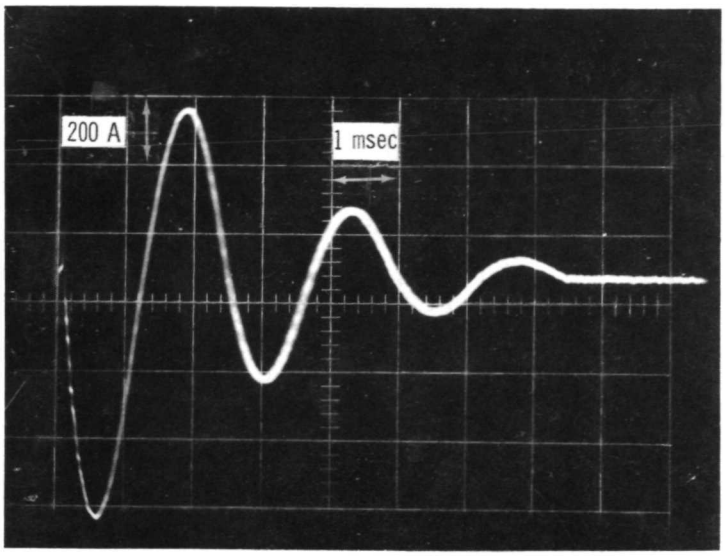

(a) Oscillograph.

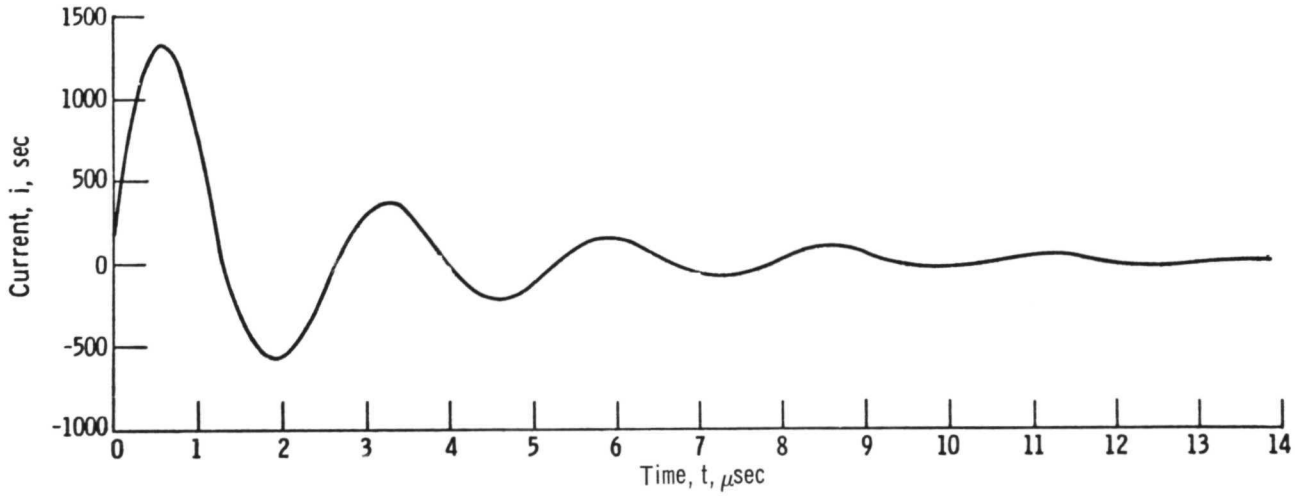

(b) Analog simulation.

Figure 36. - Current pulse occurring with 0.46-microfarad capacitance, 0.385-microhenry inductance, and 0.234 ohm resistance.

Page Intentionally Left Blank

"The aeronautical and space activities of the United States shall be conducted so as to contribute . . . to the expansion of human knowledge of phenomena in the atmosphere and space. The Administration shall provide for the widest practicable and appropriate dissemination of information concerning its activities and the results thereof."

—NATIONAL AERONAUTICS AND SPACE ACT OF 1958

NASA SCIENTIFIC AND TECHNICAL PUBLICATIONS

TECHNICAL REPORTS: Scientific and technical information considered important, complete, and a lasting contribution to existing knowledge.

TECHNICAL NOTES: Information less broad in scope but nevertheless of importance as a contribution to existing knowledge.

TECHNICAL MEMORANDUMS: Information receiving limited distribution because of preliminary data, security classification, or other reasons. Also includes conference proceedings with either limited or unlimited distribution.

CONTRACTOR REPORTS: Scientific and technical information generated under a NASA contract or grant and considered an important contribution to existing knowledge.

TECHNICAL TRANSLATIONS: Information published in a foreign language considered to merit NASA distribution in English.

SPECIAL PUBLICATIONS: Information derived from or of value to NASA activities. Publications include final reports of major projects, monographs, data compilations, handbooks, sourcebooks, and special bibliographies.

TECHNOLOGY UTILIZATION PUBLICATIONS: Information on technology used by NASA that may be of particular interest in commercial and other non-aerospace applications. Publications include Tech Briefs, Technology Utilization Reports and Technology Surveys.

Details on the availability of these publications may be obtained from:

SCIENTIFIC AND TECHNICAL INFORMATION OFFICE

NATIONAL AERONAUTICS AND SPACE ADMINISTRATION

Washington, D.C. 20546